Chinese Physics C Vol. 37, No. 6 (2013) 066001

Modeling the applicability of linear energy transfer on single event upset occurrence*

GENG Chao(耿超)[1,2;1)] LIU Jie(刘杰)[1;2)] ZHANG Zhan-Gang(张战刚)[1,2] XI Kai(习凯)[1,2]
GU Song(古松)[1,2] HOU Ming-Dong(侯明东)[1] SUN You-Mei(孙友梅)[1] DUAN Jing-Lai(段敬来)[1]
YAO Hui-Jun(姚会军)[1] MO Dan(莫丹)[1] LUO Jie(罗捷)[1]

[1] Institute of Modern Physics, Chinese Academy of Sciences, Lanzhou 730000, China
[2] University of Chinese Academy of Sciences, Beijing 100190, China

Abstract: Geant4 tools were used to model the single event upset (SEU) of static random access memory cells induced by heavy ion irradiation. Simulated results obtained in two different regions of incident ion energies have been compared in order to observe the SEU occurrence by energetic ions and their effects on the radial ionization profile of deposited energy density. The disagreement of SEU cross sections of device response and radial distribution of deposited energy density have been observed in both low energy and high energy regions with equal linear energy transfer (LET) which correspond to the both sides of the Bragg peak. In the low energy region, SEUs induced by heavy ions are more dependent upon the incident ion species and radial distribution of deposited energy density, as compared with the high energy region. In addition, the velocity effect of the incident ion in silicon in the high energy region provides valuable feedback for gaining insight into the occurrence of SEU.

Key words: SEU occurrence, LET, ion track structure, energy density

PACS: 95.75.-z, 61.82.Fk, 24.10.Lx **DOI:** 10.1088/1674-1137/37/6/066001

1 Introduction

Linear energy transfer (LET) was theorized [1] before its wide application in the domain of space radiation, cosmic ray studies, dosimetry, medical physics, and radio-biology. Currently, LET is exclusively used as the engineering metric to characterize the single event upsets (SEUs) in accelerator based testing and computational simulation. Particularly, the concept of effective LET is widely evaluated for angular incident particles on the cosine law condition. However, the analysis of SEU caused by the incident ions travelling through the sensitive volume (SV), as a function of LET has limitations. For instance, LET is a linear average over the distribution of energy loss [2], which is an important but subtle limitation of LET. Thus, the application of LET may be unsatisfactory on SEU occurrence observation and prediction, and previous studies suggest that the implications of utilizing charge deposition or critical charge in analyzing SEUs become increasingly valuable and practical.

The inadequacy of modeling SEU in static random access memory (SRAM) induced by ions of the same LET had been pointed out previously. W. J. Stapor et al. presented that more charge was collected for the higher energy ions than for the lower energy ions but with the same LET (the incident ions in the 1–100 MeV/u energy range) [3]. Afterwards, P. E. Dodd et al. further demonstrated that it possibly had a lack of correlation of the SEU cross sections with ion LET [4, 5]. As a result, the issue of fidelity of incident ion LET as an engineering metric provided by accelerator-based testing and computational simulation has been questioned because of the above results of the mentioned literature. Similarly, to distinguish it from LET, previous research predicted that SEU cross sections depend on ion species and energies [4, 6, 7]. Consequently, the probability of deposited energy in the same device structure for different ion species and energies, but all having the same LET, has been estimated in this study.

In addition, device simulation and heavy ion irradiation simulation modeling have both been used due to the flexibility and feasibility of computational simulation to study the device susceptibility to SEUs. In this work, two types of Geant 4 tools, the Monte-Carlo Radiative Energy Deposition (MRED) software package

Received 26 July 2012
* Supported by National Natural Science Foundation of China (11179003, 10975164, 10805062, 11005134)
1) E-mail: gengchao@impcas.ac.cn
2) E-mail: j.liu@impcas.ac.cn
©2013 Chinese Physical Society and the Institute of High Energy Physics of the Chinese Academy of Sciences and the Institute of Modern Physics of the Chinese Academy of Sciences and IOP Publishing Ltd

(which is based on Geant4 libraries, developed at Vanderbilt University [8, 9]) and the MUlti-Functional Package for SEEs Analysis (MUFPSA) package, have been used in the calculation of SEU characterization. In particular, the other computational method MUFPSA package also based on Geant4 (a library of C++ routines assembled by international collaboration for describing radiation interaction with matter [10]) was originally and successfully programmed by our group specially for describing and predicting the SEU occurrence by heavy ions.

In the present work, SEU measurements are used to investigate the response to variations of species and energies of the incident ions. Three types of ions, ^{131}Xe, ^{181}Ta, and ^{209}Bi having different initial energies but the same LET are used. SEU cross sections have been calculated depending on the energy deposition (or charge collection) by MERD and MUFPSA. Furthermore, a detailed understanding of the radial distribution of energy density, especially with the description of the maximum secondary particles range and velocity effect of incident ions in silicon, has been taken into consideration to analyze the simulated results from MRED and MUFPSA. In particular, as the device features continue to decrease into the nanoscale, the ion track structure profile in silicon is potentially important to study the SEU characterization in specific devices.

2 Simulation of SRAM cell

The concept of SV is derived from the Rectangular Parallelepiped (RPP) or chord model which assumes that there is a bounded region within a device named SV having the shape of a RPP. Thus, the RPP model is frequently applied for predicting the rates of SEU occurrence and analyzing the mechanism of charge deposition or collection induced by heavy ions [6–9, 11]. In this study, the SV geometry is determined for subsequent RPP based on previous work [6, 11–13] – the dimensions of the sensitive region (x, y) are 2 μm×2 μm. From the comparison of the results obtained with different SV sizes and shapes, it appears that the best approach is to use a flat SV rather than a cubic one to decrease the change in LET along an ion track in the SV [11]. Therefore, according to the literature [6, 11–13], the size of the SV is defined as 2 μm×2 μm×1 μm herein.

In order to tabulate the energy deposition and charge collection, a test structure model must be required to place the SV. To simulate more accurately, a detailed description of the device, a high resolution image of the complementary metal oxide semiconductor (CMOS) device structure including tungsten plugs and a scanning electron microscope (SEM) cross section of one kind of SRAM are illustrated in Fig. 1(a). Overall, multilevel interconnects and passivation layers together constitute the CMOS device and SRAM. Note that vias, plugs and studs are composed of tungsten, which is frequently applied in integrated circuits to provide electrical connections between layers of metallization or in contacts to the underlying silicon.

Figure 1(b) shows the vertical section of a hypothetical device representing a scaled CMOS structure. The test structure of the hypothetical device consists of silicon on insulator vertical n^{+}/p diodes fabricated by Sandia National Laboratories using CMOS7 technology but modified and optimized. As can be seen in Fig. 1(b), twelve multilayer stacks were constructed with alternating oxides and metal layers of various thicknesses, the lateral dimensions of the device structure for normally incident unidirectional beam irradiation simulations are 14 μm×14 μm. Additionally, the SV 2 μm×2 μm×1 μm silicon volume is located beneath the metallization stacks to allow rapid and convenient estimation of the SEU sensitivity.

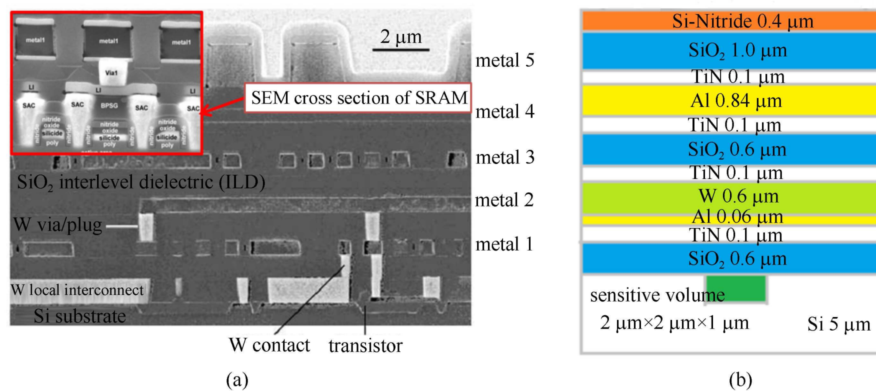

Fig. 1. (color online) (a) The high resolution image of CMOS device vertical section with multilevel interconnects and tungsten vias [14] and SEM vertical section of one kind of SRAM [12]; (b) The schematic of the metallization structure of a hypothetical device, with a surface area 14 μm×14 μm. Not drawn to scale.

3 Heavy ion irradiation simulation

The plot of heavy ion SEU cross sections versus LET as an important standardization provides valuable feedback to SEU studies and characterization. However, as previously studied, the applicability of the metric of LET may be not sufficient to ensure the observed trends in a measured SEU cross section. For example, the authors [3, 4, 7] found more than a two orders of magnitude difference in SEU cross sections. More details will be discussed in the following as shown by Fig. 2. In this work, for calculating the SEU occurrence, heavy ion irradiations are performed by the MRED and MUFPSA computational methods.

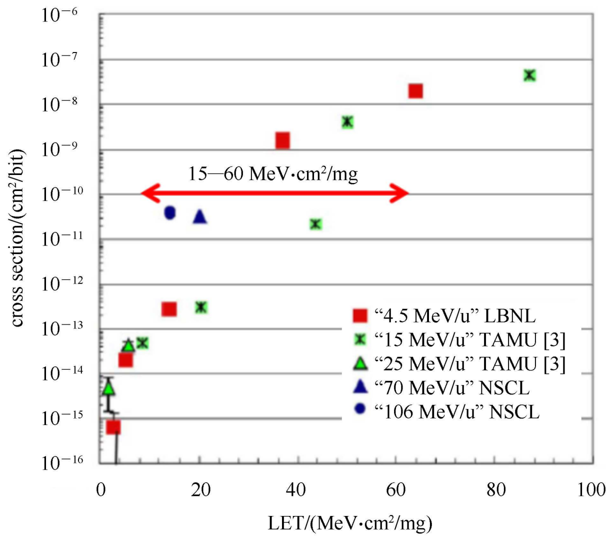

Fig. 2. (color online) The measured SEU cross sections versus the LET of normal incident ions at three different facilities [7].

It is summarized that the experimental data were taken at three different facilities, for a range of ion energies [7]. It is obviously presented in Fig. 2 that the SEU cross sections corresponding to the LET value near 15–60 MeV·cm^2/mg have more fluctuations. Moreover, the concept of effective LET should be more rigorously studied due to the angular effect on SEUs. Thus, the incident ions and the measured SEU cross sections have not given correction for incident angle in order to avoid the concept of effective LET and effective cross section.

To achieve and optimize the model of calculating the SEU cross sections, all the ion LET values taken are the stopping powers divided by silicon density for normalization. Moreover, the curves of LET vs energy for the chosen ion species should get overlapped and remarkable local gaps of energy at the abscissa in order to explicitly classify different ion energies. As instructed in Fig. 2, the LET values are selected within the range from 15 to 60 MeV·cm^2/mg.

Assuming that the calculation by using SRIM 2011 is accurate and acceptable. The LET values of incident ions in silicon are shown in Fig. 3. The energy loss was measured directly with the change of energy by SRIM 2011. As illustrated in Fig. 3, all ion species have their own Bragg peak, the maximum of energy loss as energetic ions travel along silicon. In this study, the same LET of about 50 MeV·cm^2/mg, which corresponds to two different energies in both sides of the Bragg peak for each ion species, is used, and Table 1 indicates all the data in detail.

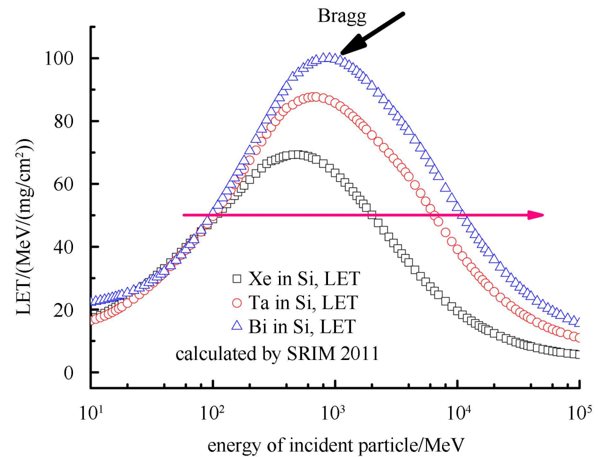

Fig. 3. (color online) The LET values of ions as a function of ion energy.

According to Table 1, the energies are classified into two groups, one is the low energy region, and the other is a high energy one. Consequently, studying the metric of the quantificational parameter LET by different species and energies of ions penetrating through the semiconductor device is more available and reasonable.

Table 1. Irradiation parameters in silicon. The incident ions have the same LET value but different energy. The ion relative velocity $\beta=v/c$, where v and c are the ion velocity and light velocity, respectively.

ions	energy/MeV	LET/(MeV/(mg/cm^2))	relative velocity	range/μm
^{131}Xe	106.71	50	0.04181	15.19
^{131}Xe	2015.64	50	0.17961	151.81
^{181}Ta	101.13	50	0.03463	14.52
^{181}Ta	6489.67	50	0.26977	435.29
^{209}Bi	97.39	50	0.03162	12.85
^{209}Bi	10981.44	50	0.32241	702.86

4 Result and discussion

4.1 The MRED and MUFPSA calculation

The incident ions based on Table 1 are mono-energetic and normally incident (to avoid the correction associated with the conception of effective LET). The incident ion is always randomly distributed on the surface of a hypothetical device, which is shown as the hypothetical device structure in Fig. 1(b). The simulated results using the same number of 10^6 incident particles at both the low energy and high energy regions are plotted in Fig. 4 as integral SEU cross sections with respect to the critical energy within the SV.

The curves in Fig. 4 demonstrate that a great discrepancy not only appears on the deposited energy, but also on the SEU cross sections. In this work, three cases will be discussed according to the simulated results from Fig. 4. First, in the case of the low energy region, the differences between the SEU cross sections induced by three low energy beams is more than one order of magnitude at the deposited energy 9 MeV. In addition, Fig. 4 shows that the incident ions with higher energy produce some larger SEU cross sections. As explained in Ref. [3], this result is probably attributed to the differences of the initial track structure; the higher energy ion's track is more spread and may yield more energy to be collected due to less initial electron-hole pair recombination.

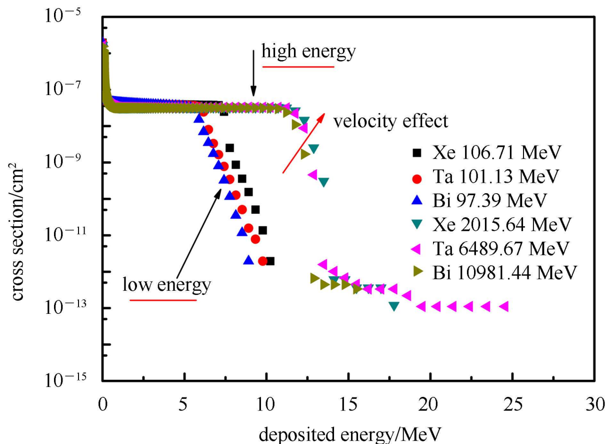

Fig. 4. (color online) The simulated integral SEU cross sections of the hypothetical device (Fig. 1) induced by ^{131}Xe, ^{181}Ta, and ^{209}Bi, at both the low energy and high energy region with the same LET value of about 50 MeV·cm^2/mg.

However, with another high energy region, the trend of SEU cross sections induced by three high energy incident beams is not the same as the low energy region. Fig. 4 shows that when the deposited energy is located at less than 12.5 MeV, the curves of high energy region as a function of deposited energy are almost consistent. However, on the condition that the maximum range of δ electrons exceeds the dimensions of cells, the relative velocities of ^{131}Xe, ^{181}Ta, and ^{209}Bi (^{131}Xe< ^{181}Ta<^{209}Bi) from Table 1 induce the decreasing trend of the initial e$^-$/h$^+$ density and hence lead to the difference of SEU cross sections (^{131}Xe>^{181}Ta>^{209}Bi) between the deposited energy 10 MeV and 12.5 MeV in Fig. 4. In addition, it is notable that the curves of SEU cross sections have a great gap of about more than two orders of magnitude of the SEU cross sections. In fact, these extended tails SEU cross sections have much smaller magnitude (10^{-13}–10^{-12} cm^2), and the energy deposition of incident ion ^{181}Ta is more than that of the highest energy incident ion ^{209}Bi. What is even worse, the highest energy ion ^{209}Bi is the least deposited energy among these ions species. It is likely that a secondary particle from the nuclear reaction between the primary ions and W, or other materials may have contributed to the above results of the extended tails' situation on SEU cross sections, even though nuclear reaction at the high energy region is less important in comparison with ionization.

The comparison between low energy and high energy regions from Fig. 4 reveals that in the higher energy region more energy is deposited. This result is more similar to the results of the case of the low energy region only. Thus it clearly demonstrates that the higher energy track is more diffuse and may yield more energy in a wider area to be collected due to less initial electron-hole pair recombination. In addition, it is also possibly attributed to the different mechanism of energy deposition by incident ions between a lower energy region (basically about atomic collision) and a higher one (mainly electronic loss). Thus, the differences of SEU cross sections only characterized by the metric of LET reveal that the applicability of LET may need to be used in a restrained manner and further studies should be carried out.

To some extent, the SEUs result from a single ion that generates charge exceeding a critical value $Q_{\rm crit}$. Therefore, $Q_{\rm crit}$ reflects the sensitivity of the SV to the collected charge, and if $Q_{\rm crit}$ is ensured, then it becomes more practical and meaningful. As a factor related to the device intrinsic characteristic, $Q_{\rm crit}$ can be given by

$$Q_{\rm crit}=\left|2\varepsilon_{\rm si}\varepsilon_0 q\left|\frac{N_{\rm D}N_{\rm A}}{N_{\rm D}+N_{\rm A}}\right|\left|\frac{K_{\rm B}T}{q}\ln\frac{N_{\rm D}N_{\rm A}}{n_{\rm i}}+V_{\rm R}\right|\right|^{1/2}S. \quad (1)$$

where ε_0 is the permittivity of vacuum, $\varepsilon_{\rm Si}$ is the relative permittivity of silicon, q is the electronic charge, $N_{\rm A}$ and $N_{\rm D}$ are the acceptor and donor impurity concentrations, $V_{\rm R}$ is the reverse bias voltage, $K_{\rm B}$ is the Boltzmann constant, T is the temperature, $n_{\rm i}$ is the intrinsic carrier concentration and S is the surface area of the SV.

Consequently, the node N^+ (or N^-) doping concentration and well (or substrate) doping concentration

have been taken as an assumption of 1×10^{20} cm^3 and 7.5×10^{19} cm^3, respectively, and $V_R=3.3$ V. In addition, the energy deposited in the SV is converted to charge using 22.5 MeV for each 1.0 pC of charge (3.6 eV needed to generate an electron-hole pair in silicon) [15] because the output of MRED and MUFPSA is energy deposition.

As shown in Fig. 5, the comparison is made between high energy and low energy induced SEU cross sections for the hypothetical device for which the critical charge is known from Eq. (1) as 7.76 MeV and the dimensions of the device geometry used are determined by Fig. 1(b). As can be seen from Fig. 5, the differences of SEU cross sections calculated both by MUFPSA and MRED at low energy region are still obvious and it is proved that almost one order of magnitude difference appears between the results. Nonetheless, for the high energy region, there is no significant discrepancy, even though different incident ions with different energies have been used. Thus, owing to the rapid development of semiconductor technology, the characteristic size of an advanced device decreases, so is the case with the critical charge related to SEU occurrence. Testing and analyzing the SEU occurrence at a low energy region should be more prudent and rigorous compared with a high energy one. Furthermore, corresponding to the mentioned results of a high energy region, it may probably need to be analyzed by the ion track profile, and the ion track profile and distribution of electron-hole pairs in silicon will be further studied.

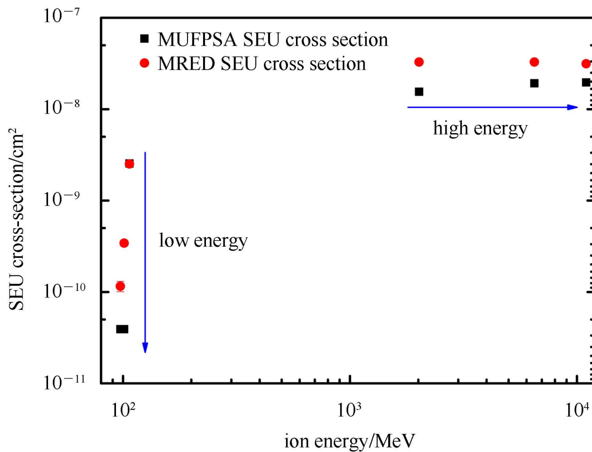

Fig. 5. The SEU cross sections induced by previously incident ions from Tab.1 traversing the hypothetical device at normal incidence are calculated by MUFPSA and MRED, respectively.

4.2 The radial ionization profile

The modeling and analysis of ion track structure response to the incident ion irradiation on arbitrary materials has been proposed in the past [16]. For SEU occurrence, the δ-ray theory of track structure is attributed to the energy deposition from the incident ions striking on the device's SV. In this work, the radial ionization profile has been successfully simulated and exhibited by MUFPSA. Additionally, the radial distribution of deposited energy density (or charge e^-/h^+ pair density) is given in Ref. [17] but optimized to be properly suited for heavy ions in silicon materials.

$$D(r)=\frac{2.84\times10^4 Z^{*2}}{\alpha\beta^2 t(t+T)}\left(\frac{R-t}{R+T}\right)^{1/\alpha}(1+K(t)),$$
$$K(t)=A\left(\frac{t-B}{C}\right)\mathrm{e}^{-\left(\frac{t-B}{C}\right)}, \tag{2}$$

where $D(r)$ is the energy density in a coaxial cylindrical shell of thickness dt at a distance from the path of an incident ion of effective Z^* moving with a relative velocity $\beta=v/c$ through silicon. In addition, $K(t)$ is the corrected expression, $B=0.1$ nm, $C=1.5$ nm$+5$ nm$\times\beta$, and $A=19\times\beta^{1/3}$.

According to the assumption of Eq. (2), the 3-D schematic diagram of the ion track structure in a cylinder with radius t induced by an incident ion as monoenergetic and normal incidence at the center of the cylinder is shown in Fig. 6(a), and the lines within the cylinder correspond to the secondary electron trajectory. Moreover, the simulated results qualitatively illustrate that at the center of the cylinder or closer to the ion path, more energy is deposited than on the boundaries. Utilizing the calculation of Eq. (2), Fig. 6(b) illustrates the radial distribution of energy density around the path of incident ions in a cylinder from quantificational analysis. The simulated results have been performed with the incident ions related to Table 1. The curves basically address the argument associated with the phenomenon of Fig. 4/5. To set radius as 1 μm for adjusting to nearly fit the SV, it illustrates that the maximum range of δ-ray is larger than the size of SV and the energy densities induced by incident ions with higher energies are mainly consistent, thus this may explain that the SEU cross sections at high energy region have little differences. Alternatively, all the curves of the low energy region demonstrate decent agreement and provide valuable feedback to correctly describe the response of the hypothetical device (SEU occurrence) to incident ions. Due to the broader radial distribution and the maximum δ-ray range smaller than the size of SV, more SEU cross sections (or energy deposition) would be induced at the low energy region as incident ions with higher energy, such as ^{131}Xe, ^{181}Ta, and ^{209}Bi in this study. As a consequence, for incident ions at the low energy region, the radial distribution of energy density has the capability of explaining the SEU characterization as a result of the entire energy deposition used for the device SEU response.

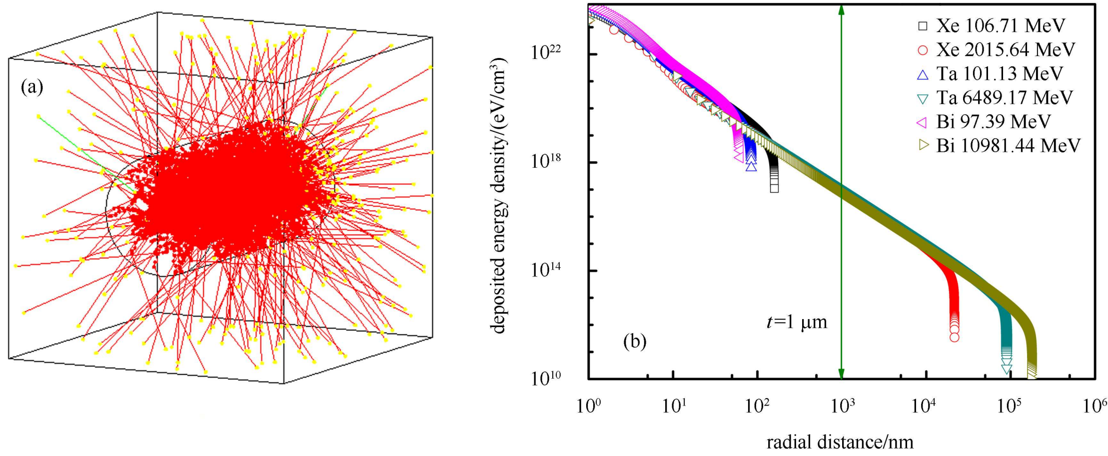

Fig. 6. (color online) The schematic of the track structure induced by incident ions traversing through silicon materials (Monte Carlo simulation) and the results of radial distribution of energy density. (a) Hypothetical cylinder within the radius t was simulated by MUFPSA, and the red ones stand for δ electrons; (b) the radial distribution of energy density around the path of incident ions in silicon.

Therefore, if the size of the SV is larger than the maximum range of δ-ray, the velocity effect of incident ions in silicon will be insignificant to SEU occurrence because all the deposited energy can contribute to the device response. However, the situation of SEU cross sections induced by incident beams at high energy region may attribute to the velocity effect of incident ions in silicon. As can be seen from Fig. 4, it is reasonably proved that the energy deposition is increasing progressively as ^{209}Bi $<^{181}$Ta $<^{131}$Xe (because higher velocity results in smaller energy density around the ion path) with respect to the marked 'velocity effect' area.

Generally, the track structure and radial distribution of energy density are strongly dependent on a function of the size and shape of the SV. Still, although the radial ionization profile can be taken as evidence of SEU characterization, this part still cannot clearly indicate the phenomenon of SEU occurrence induced by the incident ions at the region of high energy. Consequently, more experiments and computational simulation may necessitate the requirements to understand and vindicate the SEU studies, especially the high energy region.

5 Conclusion

In this work, the SEU cross sections of a hypothetical SRAM device have been calculated by MRED and MUFPSA, respectively. Under the condition of the same LET but different ion species and energies, the simulated results show that the classical single-valued LET parameter is not the only metric to characterize the SEU occurrence and its applicability may need to be further considered.

When incident beams have a maximum range of track radius smaller than the SV, irrespective of the velocity effect, similar discrepancies of simulated results of SEU cross sections emerging in the low energy region have been noted with respect to the radial distribution of energy density. In contrast, the tails of the high energy region curves may probably result from the small probability event of nuclear reaction between the incident ions and the high-Z materials of metallization layers. Fortunately, the SEU cross sections in marked 'velocity effect' areas have decent agreement with the corresponding radial distribution of energy density, and the velocity effect of incident beams in silicon has well explained the phenomenon of SEU occurrence.

Consequently, the incident ions with different energies but the same LET have some impact on energy deposition in the SRAM structure, and the simulated results show that the radial ionization profile in silicon provides effective evidence to analyze the mechanism of SEU characterization under heavy ion irradiation. In addition, it also indirectly proves that the accelerator testing with an incident beam in the low energy region is receivable and reasonable and its data still have some room to validate and support the SEU-testing and radiation hardening technology as compared with the high energy region.

References

1 McKay K G, McAfee K B. Phys. Rev., 1953, **91**: 1079–1084
2 Dicello J F, Wasiolek M, Zaider M. IEEE Trans. Nucl. Sci., 1991, **38**: 1203–1209
3 Stapor W J, McDonald P T, Knudson A R et al. IEEE Trans. Nucl. Sci., 1988, **35**: 1585–1590
4 Dodd P E, Schwank J R, Shaneyfelt M R et al. IEEE Trans. Nucl. Sci., 2007, **54**: 889–893
5 Dodd P E, Schwank J R, Shaneyfelt M R et al. IEEE Trans. Nucl. Sci., 2007, **54**: 2303–2311
6 Warren K M, Weller R A, Mendenhall M H et al. IEEE Trans. Nucl. Sci., 2005, **52**: 2125–2131
7 Reed R A, Weller R A, Mendenhall M H et al. IEEE Trans. Nucl. Sci., 2007, **54**: 2312–2321
8 Weller R A, Reed R A, Warren K M et al. IEEE Trans. Nucl. Sci., 2009, **56**: 3098–3108
9 Weller R A, Schrimpf R D, Reed R A et al. IEEE Trans. Nucl. Sci., 2010, **57**: 1726–1746
10 Agostinelli S, Allison J, Amako K et al. Nucl. Instrum. Methods Phys. Res. A, 2003, **506**: 250–303
11 Huhtinen M, Faccio F. Nucl. Instrum. Methods Phys. Res. A, 2000, **450**: 155–172
12 Warren K M. Sensitive Volume Models for Single Event Upset Analysis and Rate Prediction for Space, Atmospheric, and Terrestrial Radiation Environment (Ph. D Thesis). Tennessee: Vanderbilt University, 2010
13 Ball D R, Warren K M, Weller R A et al. IEEE. Trans. Nucl. Sci., 2006, **53**: 1794–1798
14 Loke A L S. Process Integration Issues of Low-Permittivity Dielectrics with Copper for High-Performance Interconnects (Ph. D Thesis). Stanford: Stanford University, 1999
15 Shockley W. Solid State Elec., 1961, **2**: 35–67
16 Cucinotta F A, Katz R, Wilson J W et al. Faculty Publications, Dept of Physics and Astronomy, 1996, 62
17 Waligorski M P R, Hamm R N, Katz R. Int. J. Raiat. Inst., 1986, **11**: 309–319